blood®
Regular Article

MYELOID NEOPLASIA

CBL mutations drive PI3K/AKT signaling via increased interaction with LYN and PIK3R1

Roger Belizaire,[1,2,*] Sebastian H. J. Koochaki,[2,3,*] Namrata D. Udeshi,[2] Alexis Vedder,[4] Lei Sun,[4] Tanya Svinkina,[2] Christina Hartigan,[2] Marie McConkey,[3] Veronica Kovalcik,[3] Amanuel Bizuayehu,[3] Caroline Stanclift,[2] Monica Schenone,[2] Steven A. Carr,[2] Eric Padron,[4] and Benjamin L. Ebert[3,5]

[1]Department of Pathology, Brigham and Women's Hospital, Boston, MA; [2]Broad Institute of MIT and Harvard, Cambridge, MA; [3]Department of Medical Oncology, Dana-Farber Cancer Institute, Boston, MA; [4]Department of Malignant Hematology, Moffitt Cancer Center, Tampa, FL; and [5]Howard Hughes Medical Institute, Dana-Farber Cancer Institute, Boston, MA

KEY POINTS

- **Unbiased phosphoproteomics and interactomics highlight a central role for LYN kinase in the oncogenic function of mutant CBL protein.**
- **LYN hyperactivation confers sensitivity to dasatinib in *CBL*-mutant cell lines and patient-derived CMML cells in vitro and in vivo.**

Casitas B-lineage lymphoma (*CBL*) encodes an E3 ubiquitin ligase and signaling adaptor that regulates receptor and nonreceptor tyrosine kinases. Recurrent *CBL* mutations occur in myeloid neoplasms, including 10% to 20% of chronic myelomonocytic leukemia (CMML) cases, and selectively disrupt the protein's E3 ubiquitin ligase activity. *CBL* mutations have been associated with poor prognosis, but the oncogenic mechanisms and therapeutic implications of *CBL* mutations remain incompletely understood. We combined functional assays and global mass spectrometry to define the phosphoproteome, CBL interactome, and mechanism of signaling activation in a panel of cell lines expressing an allelic series of *CBL* mutations. Our analyses revealed that increased LYN activation and interaction with mutant CBL are key drivers of enhanced CBL phosphorylation, phosphoinositide-3-kinase regulatory subunit 1 (PIK3R1) recruitment, and downstream phosphatidylinositol 3-kinase (PI3K)/AKT signaling in *CBL*-mutant cells. Signaling adaptor domains of CBL, including the tyrosine kinase–binding domain, proline-rich region, and C-terminal phosphotyrosine sites, were all required for the oncogenic function of CBL mutants. Genetic ablation or dasatinib-mediated inhibition of LYN reduced CBL phosphorylation, CBL-PIK3R1 interaction, and PI3K/AKT signaling. Furthermore, we demonstrated in vitro and in vivo antiproliferative efficacy of dasatinib in *CBL*-mutant cell lines and primary CMML. Overall, these mechanistic insights into the molecular function of *CBL* mutations provide rationale to explore the therapeutic potential of LYN inhibition in *CBL*-mutant myeloid malignancies. (*Blood*. 2021;137(16):2209-2220)

Introduction

Hematologic malignancies are often characterized by somatic alterations in genes encoding signaling proteins, leading to increased cytokine sensitivity, cell survival, and proliferation.[1] Recurrent somatic mutations in the Casitas B-lineage lymphoma (*CBL*) gene, which encodes an E3 ubiquitin ligase and signaling adaptor, occur in myelodysplastic syndromes (MDSs) and other myeloid neoplasms,[2-9] including 10% to 20% of chronic myelomonocytic leukemia (CMML) patients.[10,11] In addition, up to 20% of children diagnosed with juvenile myelomonocytic leukemia harbor germline *CBL* mutations.[12-15] The presence of *CBL* mutations has been associated with poor prognosis,[16-18] and a better understanding of the mechanisms by which *CBL* mutations promote myeloid disease is needed for the development of new and effective therapeutic strategies.

The domain structure of the CBL protein comprises an N-terminal tyrosine kinase–binding (TKB) domain followed by a linker region, RING domain, proline-rich region (PRR), C-terminal phosphorylation sites, and a ubiquitin-association domain.[19] As a signaling adaptor, CBL's TKB domain, PRR, and C-terminal phosphorylation sites facilitate coupling between tyrosine-phosphorylated cytokine receptors on the cell membrane and intracellular proteins involved in signal transduction. The RING domain, which binds E2 ubiquitin ligase proteins, and linker region are both essential for CBL's E3 ubiquitin ligase function. The majority of *CBL* mutations in myeloid malignancies are predicted to alter the ubiquitin ligase activity of CBL through single amino acid substitutions within the linker region or RING domain,[3,5-15] or splice site alterations resulting in exclusion of most amino acids within the RING domain.[15,20] Recurrent mutations predicted to affect CBL's signaling adaptor functions are exceptionally rare, implying that oncogenic *CBL* mutations result in selective loss of CBL's E3 ubiquitin ligase function. Moreover, *CBL* mutations often occur in the setting of acquired 11q uniparental disomy including the *CBL* locus, suggesting that expression of wild-type

(WT) *CBL* impairs the oncogenic phenotype in cells expressing mutant *CBL*.[3,5,6,21] Consistent with the genetics of *CBL* mutations in myeloid malignancies, missense mutations in the RING domain of murine *Cbl* promoted the development of a myeloproliferative disorder that was not observed in *Cbl*-knockout mice.[22-24] Together with work from other groups,[6,15] these data indicate that *CBL* mutations confer a gain of function associated with disruption of E3 ubiquitin ligase activity and preservation of signaling adaptor functions.[21]

Because *CBL* mutations inactivate the ubiquitin ligase activity of CBL while retaining domains needed for downstream signaling, we hypothesized that defective degradation of phosphorylated proteins causes oncogenic activation of signaling pathways; indeed, a screen of 7 tyrosine kinase inhibitors in the *CBL*-mutant cell line, GDM-1, suggested that *CBL* mutations lead to hyperactivation of a subset of signaling pathways.[25] Here, we performed unbiased and comprehensive analyses of the signaling pathways and CBL interactome in a panel of cell lines expressing an allelic series of *CBL* mutations using quantitative liquid chromatography–tandem mass spectrometry (MS). We found that the CBL–LYN–phosphatidylinositol 3-kinase (PI3K) axis[26-29] plays a significant role in the gain-of-function phenotype conferred by *CBL* mutations. In addition, LYN inhibition by dasatinib effectively diminished the expansion of *CBL*-mutant cell lines and primary CMML samples in vitro and in vivo, highlighting the potential of LYN-targeted therapies in patients with *CBL*-mutated myeloid disease.

Materials and methods

Analysis of *CBL* mutations in patient samples

Patients undergoing evaluation for various hematologic disorders (2015-2019) were consented for targeted gene sequencing using a panel developed at the Brigham and Women's Hospital and Dana-Farber Cancer Institute.[30] The frequency and type of *CBL* mutations detected in 191 deidentified patients were cataloged.

Dose response and cell-competition assays

Dose response and cell competition assays were performed as previously described.[31] Details are provided in supplemental Materials and methods (available on the *Blood* Web site).

Quantitative proteomics and phosphoproteomics

The experimental setup for quantitative proteomics/phosphoproteomics and CBL interaction proteomics are presented in supplemental Tables 1 and 5, respectively. Details are provided in supplemental Materials and methods.

Western blot

Detailed descriptions of protein lysate preparation, immunoprecipitation (IP), electrophoresis, western blot (WB) protocol, and antibodies are provided in supplemental Materials and methods.

CMML colony-forming assays and xenotransplantation experiments

Colony-forming assays and xenotransplantation assays were performed as previously described.[32] Details are provided in supplemental Materials and methods.

Graphs, tables, and figures

Graphs were generated using GraphPad Prism version 7 (San Diego, CA). Morpheus software (https://software.broadinstitute.org/morpheus) was used to perform nearest-neighbor analysis and generate heatmap and statistics (see Figure 3A). Tables were generated in Microsoft Excel or PowerPoint (Redmond, WA). Figures were prepared using Microsoft PowerPoint.

Results

Characteristics of *CBL* mutations in 191 patients

To select common, recurrent *CBL* mutations for functional studies, we examined clinical sequencing data from 9122 patients undergoing evaluation for hematologic disorders, including MDSs and myeloid leukemias.[30] Two hundred fourteen *CBL* mutations were detected (supplemental Figure 1A), of which 195 (91%) were single-nucleotide changes leading to amino acid substitutions predicted to disrupt the function of the linker region or RING domain (supplemental Figure 1B). Overall, single amino acid substitutions at positions Y371, L380, C384, C404, and R420 were most common, comprising nearly 50% of all *CBL* mutations (supplemental Figure 1C).

CBL mutations activate LYN and PI3K/AKT-signaling pathways

To elucidate the mechanisms by which mutant *CBL* promotes myeloid oncogenesis, we generated an allelic series of *CBL* mutations that reflects the genetics of human myeloid malignancies in cytokine-dependent cell lines. We focused on our analysis of 3 common *CBL* missense mutations: 1 that occurs within the linker region (Y371H) and 2 that occur within the RING domain (C384Y and R420Q). To generate an in vitro model consistent with the observed 11q uniparental disomy observed in patients with *CBL* mutations,[3,5,6,21] we first used clustered regularly interspaced short palindromic repeats (CRISPR)–CRISPR-associated protein 9 (Cas9) to produce *Cbl*-knockout clones in the murine myeloblast cell line, 32D (supplemental Figure 2), which proliferates in response to either interleukin 3 (IL3) or granulocyte-macrophage colony-stimulating factor (GM-CSF). To investigate the effects of *CBL* mutations on cytokine signaling and proliferation, we next generated a panel of cell lines overexpressing human, V5-tagged, mutant (ie, Y371H, C384Y, or R420Q) or WT *CBL* in 32D-Cbl^{KO} cells (supplemental Figure 3). Compared with expression of *CBL* WT, expression of *CBL* mutants was associated with increased IL3 and GM-CSF sensitivity in cell-proliferation assays (Figure 1A-B; supplemental Table 1); expression of the same *CBL* mutants in the murine lymphoblast cell line BaF3 also led to increased IL3 sensitivity and was sufficient to promote IL3 independence (Figure 1C; supplemental Figure 4).

To determine whether cells expressing *CBL* mutants had a competitive advantage over cells expressing *CBL* WT, we cocultured green fluorescent protein (GFP)-labeled *CBL*-mutant cells with dTomato-labeled *CBL* WT cells at a ratio of 1:10 in limiting IL3 (0.1 ng/mL) and performed serial measurements of the GFP:dTomato ratio using flow cytometry. For each *CBL* mutant tested, the GFP:dTomato ratio increased significantly over several days, indicating that expression of *CBL* mutants conferred a proliferative advantage (Figure 1D); similar results were observed in the GM-CSF–dependent human cell line TF1 and in BaF3 (Figure 1E; supplemental Figure 4B). Cells expressing *CBL*

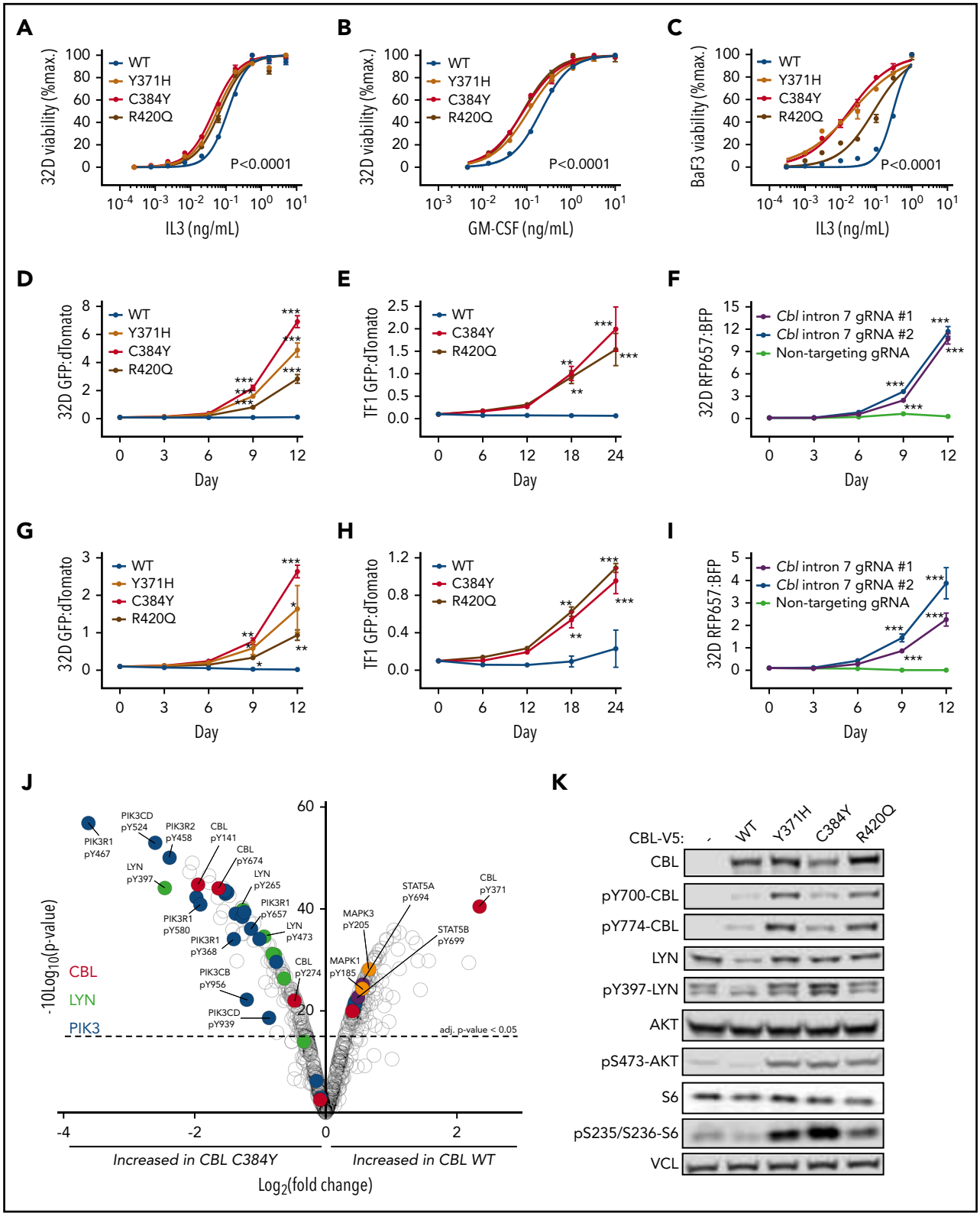

Figure 1. Gain-of-function *CBL* mutations are associated with increased cytokine sensitivity and activation of the LYN and PI3K/AKT-signaling pathway. (A-C) Proliferation of *Cbl*^{KO} 32D (A-B) or BaF3 (C) cells expressing WT or mutant CBL after 3-day stimulation with IL3 (A,C) or GM-CSF (B). (D-I) Competition between GFP-labeled 32D-*Cbl*^{KO} (D,G) or TF1-*CBL*^{KO} (E,H) cells expressing CBL-mutant and dTomato-labeled CBL WT (D-E) or CBL knockout (KO) (G-H) cells. Competition between 32D-Cas9 cells expressing *Cbl* intron 7 guide RNAs (gRNAs) (RFP657) and nontargeting gRNA (blue fluorescent protein [BFP]; panel F) or *Cbl* exon 1 gRNAs (BFP; panel I). (J) Volcano plot showing relative quantity of phosphotyrosine sites detected by MS and normalized to proteome-level data in 32D-*Cbl*^{KO} cells expressing V5-tagged CBL WT or C384Y. (K) WB for total and phosphorylated CBL, LYN, AKT, and S6 proteins in 32D-*Cbl*^{KO} cells expressing V5-tagged CBL WT, Y371H, C384Y, or R420Q. WB for vinculin (VCL) was used as a loading control. Statistical significance for cytokine dose-response curves was determined by a 2-tailed Student *t* test comparing the 50% effective concentration for each CBL mutant with CBL WT (see also supplemental Table 1). Statistical significance for competitive proliferation assays was determined by 2-tailed Student *t* test comparing each CBL mutant with CBL WT or KO (*$P < .05$; **$P < .001$; ***$P < .0001$).

mutants also displayed a proliferative advantage over cells with complete loss of *CBL* (ie, 32D-*Cbl*^{KO} or TF1-*CBL*^{KO}), consistent with the expected gain of function of the CBL-mutant protein (Figure 1G-H). Finally, CRISPR-Cas9–mediated editing of endogenous *Cbl* exon 8 splice sites in 32D cells led to exon 8 exclusion, similar to *CBL* exon 8 splice-site mutations in human myeloid disease,[15,20] as well as increased cell proliferation compared with both *Cbl*^{WT} and *Cbl*^{KO} 32D cells (supplemental Figure 5; Figure 1F,I). Altogether, these mouse and human cell lines model myeloid disease–associated *CBL* mutations by demonstrating that selective disruption of CBL's linker region or RING domain leads to gain-of-function effects on cytokine sensitivity and cell proliferation.

We leveraged our in vitro models of *CBL* mutations to explore the signaling pathways that are activated in *CBL*-mutant cells. Given the role of CBL in cytokine receptor signaling,[19] we used quantitative MS with tandem mass tags and antibody-based enrichment of tyrosine-phosphorylated peptides. Global tyrosine phosphorylation in 32D-*Cbl*^{KO} cells expressing CBL WT or CBL C384Y, cultured in limiting IL3 (0.1 ng/mL), was characterized to highlight the constitutively activated pathways in CBL C384Y cells. The global proteome as well as phosphoserine (pS) and phosphothreonine (pT) peptides were quantitated in parallel in the same samples (supplemental Tables 2-7). Among proteins detected in both global and phosphoproteomic data sets, we found no significant differences in the global proteome or proteome-normalized pS and pT peptides between cells expressing CBL WT and CBL C384Y. In contrast, we found that proteome-normalized tyrosine phosphorylation of CBL, LYN, and multiple proteins in the PI3K-signaling pathway (eg, phosphoinositide-3-kinase regulatory subunit 1/2 [PIK3R1/2], phosphatidylinositol-4,5-bisphosphate 3-kinase catalytic subunit β/δ [PIK3CB/D], and phosphoinositide-3-kinase adaptor protein 1 [PIK3AP1]) were significantly increased in cells expressing CBL C384Y compared with CBL WT (Figure 1J). Phosphorylation of LYN, an SRC family kinase, on tyrosine 397 (pY397), was among the most significantly increased phosphotyrosine sites in CBL C384Y cells, and has been shown to stimulate LYN-kinase activity.[33] Changes in tyrosine phosphorylation that would indicate activation of the MAPK or JAK-STAT pathways were not observed in cells expressing CBL C384Y. Notably, MAPK1 pY185 and MAPK3 pY205, which indicate MAPK-pathway activation, and STAT5A pY694 and STAT5B pY699, which indicate JAK activity, were significantly reduced in cells expressing mutant C384Y (Figure 1J). Thus, our MS-based analysis of tyrosine phosphorylation implicated a CBL-LYN-PI3K axis in the enhanced cell proliferation associated with expression of mutant *CBL* in 32D cells.

To determine whether LYN kinase activation was a common feature of *CBL*-mutant expression, we measured LYN pY397 by WB in cells expressing a series of mutant *CBL* alleles. In line with our phosphoproteomic results, LYN pY397 levels were increased in cells expressing *CBL* mutants compared with *CBL* WT (Figure 1K; supplemental Figure 6). Total LYN protein was also increased in *CBL*-mutant cell lines. Consistent with enhanced LYN activation, WB analysis of 32D and TF1 cells expressing *CBL* mutants also revealed increased CBL phosphorylation at known LYN target sites Y700 and Y774.[26] Our global proteomic analysis also demonstrated a significant increase in tyrosine phosphorylation of PI3K-associated proteins, suggestive of increased signaling in the PI3K pathway, although the biological roles of the specific phosphotyrosine sites that were detected have not been reported. We therefore used WB to measure AKT pS473 and ribosomal S6 pS235/236, which are directly indicative of signaling in the PI3K pathway. Indeed, phosphorylation of AKT and ribosomal S6 were increased in *CBL*-mutant cells compared with *CBL* WT cells (Figure 1K; supplemental Figure 6). AKT and S6 phosphorylation were unchanged in 32D-*Cbl*^{KO} cells even though LYN protein and phosphorylation were increased compared with 32D-*Cbl*^{WT} cells, highlighting that expression of CBL-mutant protein was required for increased PI3K/AKT signaling; this finding also implies that the expression of *CBL* WT, but not mutant, leads to reduced LYN protein and phosphorylation. ERK and STAT5 phosphorylation were unchanged or reduced in 32D cells expressing *CBL* mutants compared with *CBL* WT, which matched our global phosphoproteomic results (supplemental Figure 7). Altogether, these data indicate that gain-of-function *CBL* mutants are associated with increased LYN-kinase activity, CBL phosphorylation, and activation of the PI3K/AKT-signaling pathway.

CBL mutants enhance cytokine signaling and cell proliferation via increased interaction with LYN

CBL mutations in myeloid malignancies disrupt the RING domain, and therefore E3 ubiquitin ligase function, whereas the adaptor domains, including the TKB domain, PRR, and C-terminal tyrosine-phosphorylation sites, remain intact.[21] Thus, we hypothesized that the functions of CBL adaptor domains play a functional role in the increased cytokine signaling and cell proliferation in *CBL* mutant–expressing cells. To explore this possibility, we generated GFP-labeled double mutants comprising the C384Y RING domain mutation with secondary mutations in the TKB domain (G306E), PRR (Δ477-688), or C-terminal phosphotyrosine sites (Y700/731/774F) in 32D-*Cbl*^{KO} cells (Figure 2A). Single and double-mutant cells were mixed with dTomato-labeled *CBL* WT cells at a ratio of 1:10, and the GFP:dTomato ratio was measured by flow cytometry to assess for the relative rates of cell proliferation. The competitive advantage of cells expressing CBL C384Y was significantly reduced with mutation of the TKB domain, PRR, or phosphotyrosine residues, indicating that CBL's adaptor domains are critical for the proliferative advantage of cells expressing mutant *CBL* (Figure 2B).

Based on the key role of CBL adaptor domains in the proliferative advantage of cells expressing *CBL* mutants, we hypothesized that CBL adaptor domains promote increased cytokine sensitivity via specific protein-protein interactions with these domains. To address this possibility, we used IP followed by MS (IP-MS) to characterize the global CBL interactome in 32D-*Cbl*^{KO} cells expressing V5-tagged CBL WT or mutants Y371H, C384Y, or R420Q (supplemental Tables 6 and 7). Comparison of the WT and mutant CBL interactomes revealed significantly increased binding of LYN to CBL mutants compared with CBL WT (Figure 2C), and we confirmed this finding by IP followed by WB (IP-WB) in both 32D and TF1 cell lines (Figure 2D; supplemental Figure 8). To define the CBL adaptor domain(s) required for the interaction between mutant CBL and LYN, we performed additional IP-WB experiments using 32D-*Cbl*^{KO} cells expressing the CBL C384Y RING domain mutant with secondary mutations in the TKB domain, PRR, or C-terminal phosphotyrosine sites. Secondary mutation of only the PRR abolished LYN binding to CBL C384Y, whereas mutations in the TKB domain or

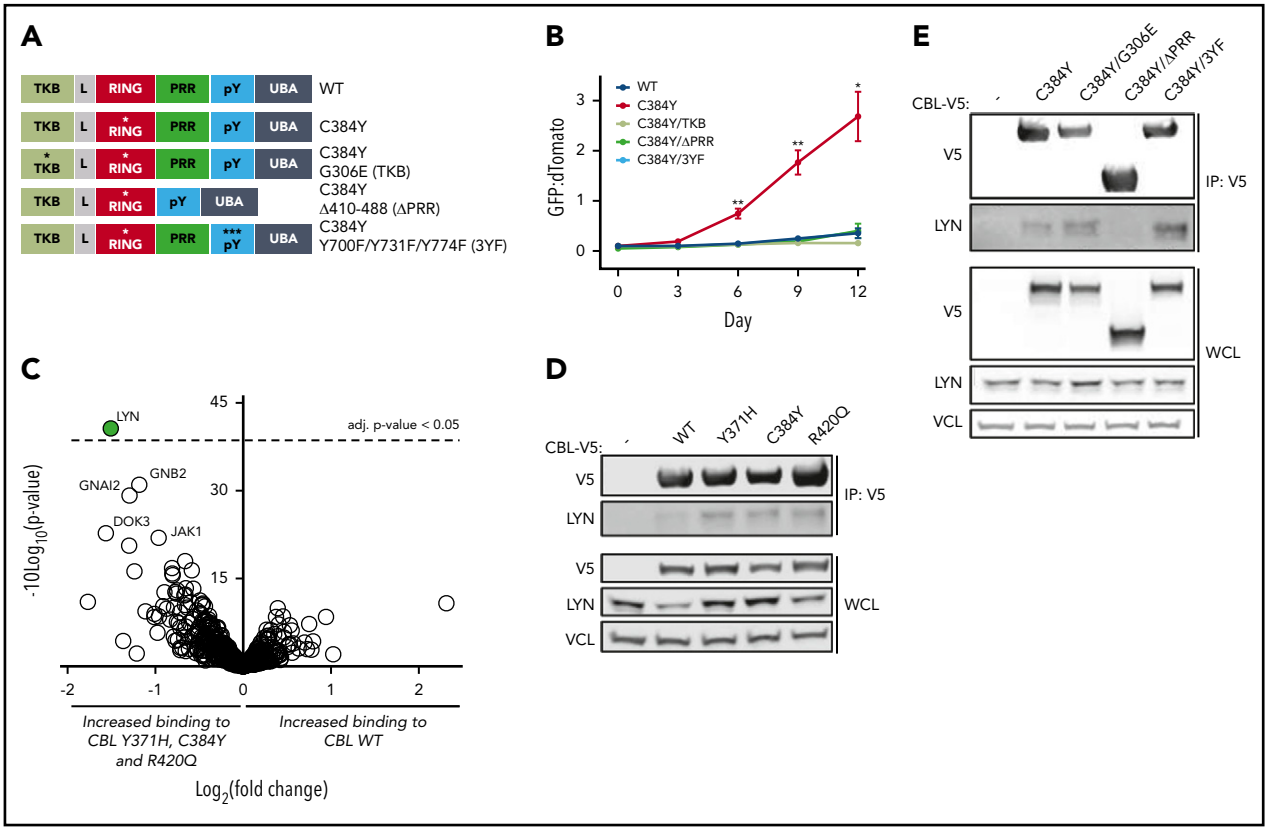

Figure 2. LYN binding to the PRR of CBL is enhanced in cells expressing CBL mutants. (A) Schematic of CBL variants with mutation of the RING domain (C384Y) in combination with the TKB domain (G306E), PRR (ΔPRR), or C-terminal phosphotyrosine sites (Y700F/Y731F/Y774F). RING domain and phosphotyrosine site mutations are indicated by asterisks. (B) Competition between CBL WT (dTomato) and CBL double mutants (GFP) expressed in 32D-*Cbl*^{KO} cells. Mean and standard deviation (SD) of triplicate values are depicted. Statistical significance was determined by 2-tailed Student *t* test comparing CBL C384Y to CBL WT and each CBL double mutant (*$P < .05$; **$P < .001$). (C) MS analysis of V5 IP samples from 32D-*Cbl*^{KO} cells expressing V5-tagged CBL WT, Y371H, C384Y, or R420Q. Volcano plot showing $\log_{10}$ *P* values and $\log_2$ fold change in protein abundance between CBL mutants (pooled data from Y371H, C384Y, and R420Q) and CBL WT samples. (D) WB for V5, LYN, and vinculin (VCL) in anti-V5 IP samples and whole-cell lysates (WCL) from 32D-*Cbl*^{KO} cells expressing V5-tagged CBL WT, Y371H, C384Y, and R420Q. (E) WB for V5, LYN, and vinculin (VCL) in anti-V5 IP samples and whole-cell lysates from 32D-*Cbl*^{KO} cells expressing V5-tagged CBL WT, C384Y, C384Y/G306E, C384Y/ΔPRR, or C384Y/3YF. L, linker; pY, phosphotyrosine; UBA, ubiquitin-associated.

C-terminal phosphotyrosine sites had no effect (Figure 2E). Similar results were obtained in TF1 cells (supplemental Figure 8). Overall, our global proteomic analyses demonstrated that enhanced proliferation of cells expressing *CBL* mutants was associated with increased LYN kinase activation and LYN protein levels, and interaction of LYN with mutant CBL.

LYN interaction with mutant CBL increases PIK3R1 recruitment and downstream PI3K/AKT signaling

To explore the role of increased CBL-LYN interaction in *CBL*-mutant cell lines, we sought to identify proteins with differential interaction with CBL in the context of LYN binding. In a nearest-neighbors analysis of our CBL IP-MS data to identify proteins with a pattern of binding most similar to LYN, the PI3K-signaling adaptor protein PIK3R1 was among the top hits. Moreover, tyrosine phosphorylation of PIK3R1 was markedly increased in CBL C384Y-expressing cells compared with CBL WT-expressing cells. IP of V5-tagged CBL followed by WB for PIK3R1 confirmed that CBL mutants Y371H, C384Y, and R420Q bound significantly more PIK3R1 compared with CBL WT (Figure 3B). Consistent with previous studies,[34,35] CBL C384Y with a secondary Y731F mutation was unable to bind PIK3R1 in both 32D and TF1 cells, indicating that tyrosine phosphorylation at position 731 of mutant CBL was essential for the interaction with PIK3R1 (Figure 3C-D). Deletion of CBL's PRR, which was required for the CBL-LYN interaction, also led to a significant decrease in the CBL-PIK3R1 interaction (Figure 3C), suggesting a potential connection between the CBL-LYN interaction and increased PIK3R1 binding. Indeed, the interaction between PIK3R1 and V5-tagged CBL C384Y was also reduced in *Lyn*-knockout 32D cells engineered by CRISPR-Cas9–mediated gene editing (Figure 3E). Thus, increased CBL-LYN interaction enhances the binding of the PI3K-signaling adaptor PI3KR1 to CBL phosphotyrosine Y731.

To test whether LYN was required for increased cell proliferation driven by CBL mutants, we compared the competitive advantage of CBL C384Y-expressing cells in *Lyn* WT and knockout 32D cells. In competition against CBL WT-expressing cells, the proliferative advantage of CBL C384Y-expressing cells was reduced by *Lyn* knockout (Figure 3F). In line with this result, *Lyn*-knockout cells expressing CBL C384Y were at a competitive disadvantage when cocultured with *Lyn* WT cells expressing CBL C384Y (supplemental Figure 9). Moreover, *Lyn* knockout was associated with reduced phosphorylation of CBL and AKT in CBL C384Y-expressing cells (supplemental Figure 10). Altogether, these experiments suggest that LYN drives proliferation of cells expressing mutant CBL via increased CBL phosphorylation, PIK3R1 recruitment, and downstream PI3K/AKT signaling.

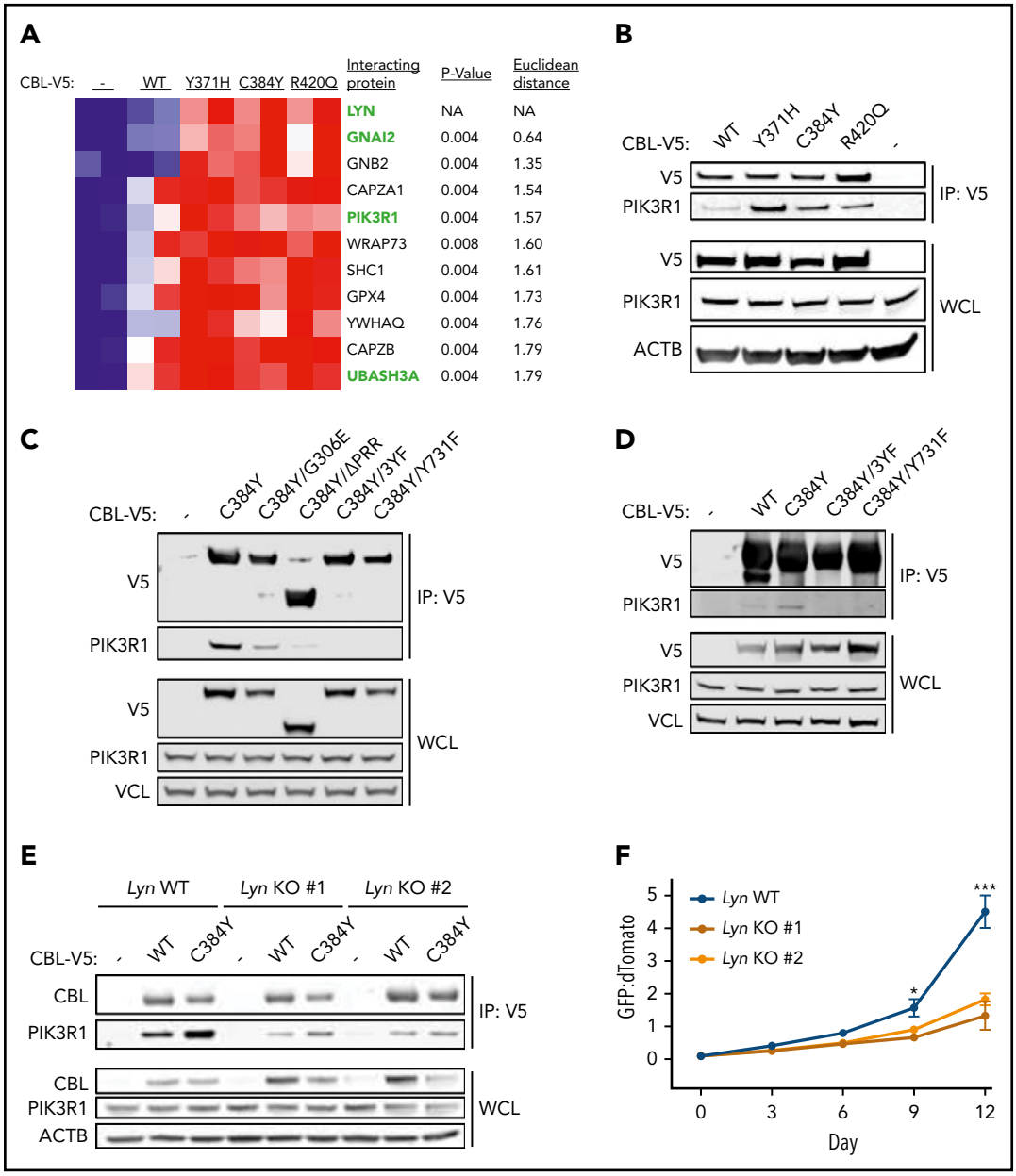

Figure 3. LYN facilitates CBL-PIK3R1 interaction and increased proliferation of CBL mutant cells. (A) Heatmap depicting relative protein abundance in V5 IP samples analyzed by MS. Top 10 proteins correlated with LYN by nearest-neighbors analysis are shown. Proteins highlighted in green also showed significantly increased tyrosine phosphorylation in 32D cells expressing CBL C384Y compared with CBL WT. (B-C) WB for V5, PIK3R1, and β-actin (ACTB) in anti-V5 IP samples and whole-cell lysates (WCL) from 32D-*Cbl*^{KO} cells expressing V5-tagged (B) CBL WT, Y371H, C384Y, and R420Q or (C) CBL WT, C384Y, C384Y/G306E, C384Y/ΔPRR, C384Y/3YF, or C384Y/Y731F. (D) WB for V5, PIK3R1, and VCL in anti-V5 IP samples and WCL from TF1-*CBL*^{KO} cells expressing V5-tagged CBL WT, C384Y, C384Y/3YF, or C384Y/Y731F. (E) WB for V5, PIK3R1, and β-actin in anti-V5 IP samples and WCL from 32D-*Lyn*^{KO} cells expressing V5-tagged CBL WT or C384Y. (F) Competition between CBL WT (dTomato) and C384Y (GFP)-expressing 32D cells on *Lyn*^{WT} and *Lyn*^{KO} genetic backgrounds. Mean and SD of triplicate values are depicted. Statistical significance for competitive proliferation assays was determined by 2-tailed Student *t* test comparing *Lyn* WT to each *Lyn* KO (*$P < .05$; ***$P < .0001$).

Dasatinib inhibits LYN activation, PI3K signaling, and proliferation in cells expressing *CBL* mutants

Given the central role of LYN in cytokine signaling downstream of CBL mutants, we hypothesized that cells expressing *CBL* mutants would be susceptible to pharmacologic inhibition of LYN. Dasatinib is a drug that inhibits ABL- and SRC-family kinases, including LYN.[36] In proliferation assays, we found that the 50% inhibitory concentration of dasatinib was lower in 32D and TF1 cells expressing CBL mutants compared with CBL WT (Figure 4A; supplemental Figure 11A; supplemental Table 8). Dasatinib also blocked the proliferative advantage of 32D cells expressing CBL Y371H, C384Y, and R420Q in competition assays (Figure 4B-D). Similar results were observed in TF1 cells and 32D cells with CRISPR-Cas9–mediated editing of *Cbl* exon 8 splice sites (supplemental Figure 11B-E). The inhibitory effect of dasatinib on proliferation of *CBL*-mutant cell lines correlated directly with decreased phosphorylation of LYN, CBL, AKT, and S6, as measured by WB (Figure 4E;

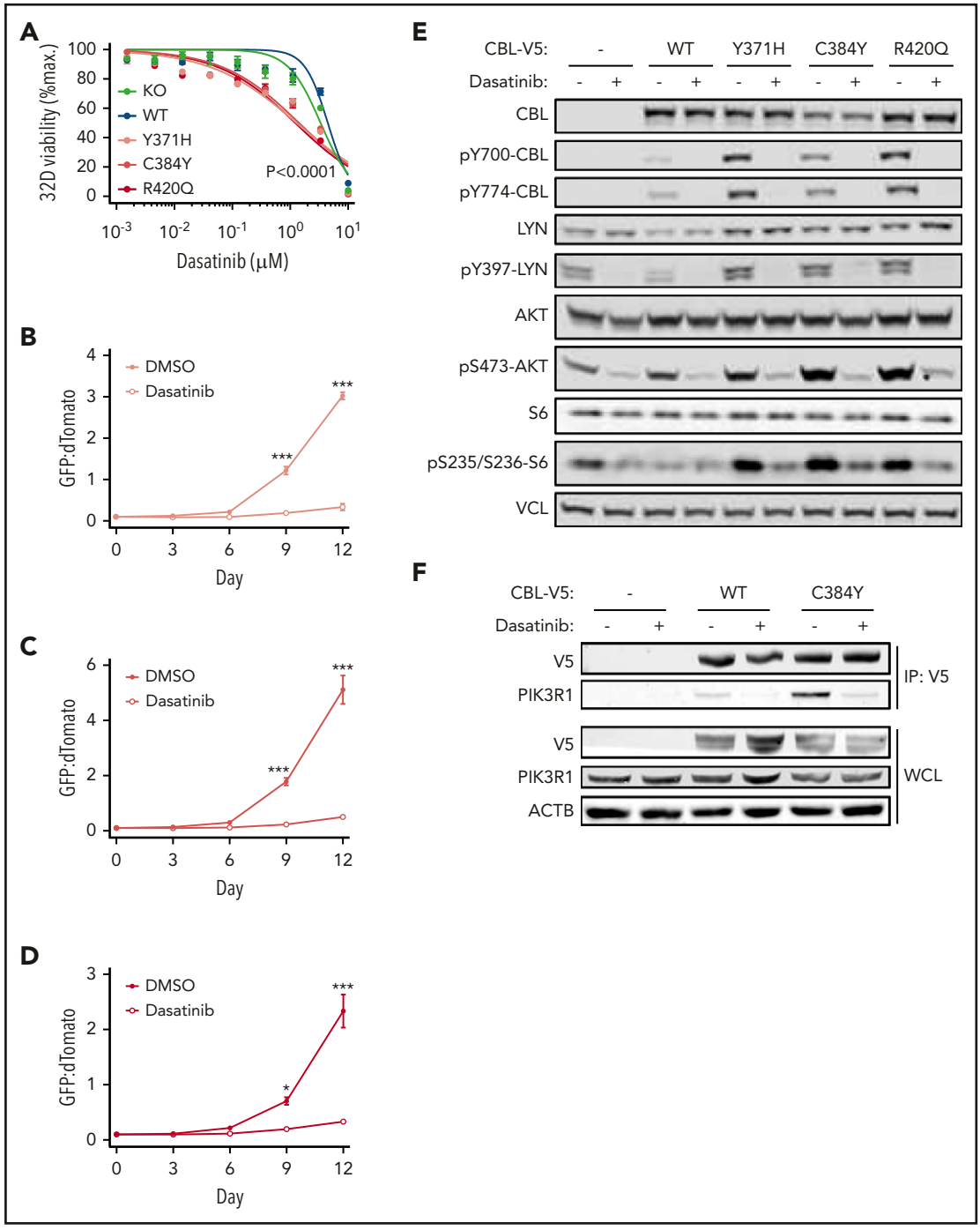

Figure 4. Dasatinib inhibits proliferation, CBL phosphorylation, PI3K/AKT signaling, and CBL-PIK3R1 interaction in *CBL*-mutant cell lines. (A) Proliferation of 32D-*Cbl*^{KO} cells expressing luciferase (KO) or V5-tagged CBL WT, Y371H, C384Y, or R420Q in the presence of DMSO or a range of dasatinib concentrations over 3 days. (B-D) Competition between dTomato-labeled 32D-*Cbl*^{KO} cells expressing CBL WT and GFP-labeled 32D-*Cbl*^{KO} cells expressing (B) CBL Y371H, (C) CBL C384Y, or (D) CBL R420Q in the presence of DMSO (closed symbols) or 1 μM dasatinib (open symbols). (E) WB for total and phosphorylated CBL, LYN, AKT, and S6 proteins in 32D-*Cbl*^{KO} cells expressing luciferase (–) or V5-tagged CBL WT, Y371H, C384Y, or R420Q treated with DMSO or 1 μM dasatinib for 2 hours. WB for vinculin (VCL) was used as a loading control. (F) WB for V5, PIK3R1, and β-actin (ACTB) in anti-V5 IP samples and WCL from DMSO- or dasatinib-treated (1 μM for 2 hours) 32D-*Cbl*^{KO} cells expressing luciferase (−) or V5-tagged CBL WT or C384Y. Statistical significance for dasatinib dose-response curves was determined by 2-tailed Student *t* test comparing the 50% inhibitory concentration for each CBL mutant to CBL WT or KO (see also supplemental Table 8). Statistical significance for competitive proliferation assays was determined by 2-tailed Student *t* test (*$P < .05$; ***$P < .0001$).

supplemental Figure 12). Moreover, dasatinib treatment abrogated the interaction between mutant CBL and PIK3R1 (Figure 4F). Overall, these results demonstrated that dasatinib inhibited the effects of *CBL* mutants on cytokine signaling and cell proliferation.

The competitive advantage of *CBL*-mutant cells was impaired but still detectable on a *Lyn*-knockout genetic background (Figure 3F), indicating the presence of other contributors to the phenotype conferred by *CBL* gain-of-function mutations. To test whether these pathways involved another SRC-family kinase

member, we assessed the effect of dasatinib on the proliferative advantage of 32D *Lyn*-knockout cells expressing CBL C384Y. Remarkably, *Lyn* knockout rendered CBL C384Y-expressing cells completely insensitive to dasatinib treatment, implying that the reduction in proliferation of *CBL*-mutant 32D cells treated with dasatinib was due to LYN inhibition (supplemental Figure 13).

Dasatinib inhibits clonogenicity and engraftment of *CBL*-mutated CMML patient samples in vitro and in vivo

We next sought to test the efficacy of dasatinib on *CBL*-mutant leukemic cells from patients with CMML. We assessed 4 *CBL*-mutated patient samples in in vitro colony-forming assays and in vivo xenograft studies (Figure 5A).[32] Up to 9 xenograft models were generated per patient and randomized to receive 10 days of 50 mg/kg dasatinib or vehicle control 2 to 4 weeks after transplantation. Samples harbored *CBL* mutations in combination with a variety of other mutations frequently seen in CMML (Figure 5B; supplemental Tables 9 and 10). All samples were from patients with myeloproliferative features and splenomegaly consistent with the clinical presentation of *CBL*-mutated CMML (supplemental Table 11). Dasatinib reduced colony formation compared with dimethyl sulfoxide (DMSO) treatment in samples from all 4 patients (Figure 5C-D). At 250 nM dasatinib, the decrease in colony formation was statistically significant in 4 of 6 samples tested (Figure 5C; supplemental Figures 14B and 16C-D). In 1 of 2 samples tested over a range of dasatinib concentrations, clonogenic growth was inhibited at 25, 50, and 100 nM dasatinib (supplemental Figure 16D; $P < .0001$ at all concentrations compared with DMSO). For *CBL*-mutant CMML samples 1, 2, and 4, dasatinib treatment of xenografted NSG-S mice was associated with a trend toward decreased splenic disease burden as measured by the percentage of human CD45$^+$ cells detected by flow cytometry and immunohistochemistry (Figure 5E-F). The decrease in splenic disease burden with dasatinib treatment was statistically significant in models generated with 2 of 4 samples. In mice xenografted with CMML sample 3, dasatinib was associated with a significant decrease in spleen weight but had a limited effect on the percentage of human CD45$^+$ cells in the spleen and bone marrow (supplemental Figure 14A-F). We also tested the effect of dasatinib on in vitro clonogenicity and in vivo expansion of patient-derived CMML samples without *CBL* mutations (supplemental Tables 10 and 13). Interestingly, dasatinib also showed activity against *CBL* WT CMML in 1 of 2 samples tested in vitro (supplemental Figure 16A-B) and 2 of 4 samples used to generate in vivo models (supplemental Figure 15). Altogether, these experiments indicated that dasatinib effectively reduced the growth of patient-derived CMML samples in vitro and in vivo.

Discussion

We used phosphoproteomics, IP-MS, and functional analyses to identify signaling pathways that drive proliferation in a panel of cell lines expressing an allelic series of *CBL* mutations. This unbiased approach highlighted a mechanism whereby increased LYN activity and binding to mutant CBL enhances CBL tyrosine phosphorylation, PIK3R1 recruitment, and downstream PI3K/AKT activation. In addition to defining this molecular pathway, our findings point to the therapeutic efficacy of LYN inhibition by dasatinib, which we validated in both cell lines and primary leukemia samples in vitro and in vivo.

CBL mutations in human myeloid malignancies selectively affect the protein's E3 ubiquitin ligase function, suggesting that CBL's role as a signaling adaptor is critical to the gain of function conferred by the mutant protein.[21] Indeed, a prior study reported that the adaptor domains of mutant CBL were essential for increased signaling and cell proliferation,[37] although the molecular basis for this finding was not fully addressed. Previous work by Ohh and colleagues indicated that increased SRC-family kinase activity was associated with increased CSF2RB phosphorylation, PI3K signaling, and reduced apoptosis in cells expressing CBL Y371H.[29,38] Using IP-MS as an unbiased discovery tool, we identified and characterized the interaction between CBL and LYN[26-28] as an important component of oncogenic signaling driven by the PRR of mutant CBL. We found an increase in total and activated LYN in both *CBL*-knockout and gain-of-function mutant cell lines, suggesting that CBL's E3 ubiquitin ligase function plays a role in regulation of LYN protein levels. We provide several lines of evidence that gain-of-function *CBL* mutations, unlike *CBL* knockout, specifically exploit LYN-kinase activity to enhance downstream PI3K/AKT signaling.

Unlike other studies that observed hyperactivation of MAPK, JAK-STAT, and PI3K/AKT pathways,[2,6,15,23,24,29,37-43] our global characterization of tyrosine phosphorylation in cells expressing mutant *CBL* revealed selective activation of LYN and the PI3K/AKT pathway. In fact, tyrosine-phosphorylation sites that directly indicate activation of the MAPK or STAT5 pathways were lower in our *CBL*-mutant cells by MS analysis; this observation could be related to the level of *CBL*-mutant expression, which was significantly higher than endogenous *Cbl/CBL* expression in our cell-line models, and resultant negative feedback. However, there are several other potential explanations for this discrepancy. First, most previous studies measured phosphosignaling using starve-stimulation assays, which provide an estimate of phosphorylation kinetics upon acute cytokine exposure.[2,6,15,23,29,37-43] Here, we performed an unbiased assessment of tyrosine phosphorylation during chronic cytokine exposure in order to identify signaling pathways that were activated and targetable in the steady state. Second, the effects of *CBL* mutations may depend on the cellular context. Along these lines, hematopoietic stem and progenitor cells from *Cbl*-mutant mice showed increased PI3K/AKT, MAPK, and STAT5 signaling, although there were differences in the signaling effects depending on the subpopulation analyzed.[24] Third, 2 studies evaluated the effects of CBL mutants on a *Cbl*$^{-/-}$/*Cblb*$^{-/-}$ genetic background,[37,43] which has the potential to augment or alter the signaling phenotype conferred by CBL-mutant protein due to functional redundancy between *Cbl* and *Cblb* in mice.[44-46] In patients with myeloid malignancies, *CBLB* mutations are uncommon and comutation of *CBL* and *CBLB* has not been described, suggesting that recurrent mutations in *CBLB* do not contribute significantly to oncogenesis. Although it is possible that *CBLB* modulates cytokine signaling in our cell-line models, we performed our analyses of *CBL* mutations in *CBLB* WT cells to accurately recapitulate human disease genetics. Fourth, the diversity of signaling adaptors and kinases associated with different cytokine receptors may determine which signaling pathways are affected by *CBL* mutations. Variability in the magnitude of the effect and pathway specificity could reflect differences in the role of mutant CBL downstream of FLT3, KIT, MPL, and receptors utilizing the common β-chain CD131 (ie, receptors for IL3, IL5, and GM-CSF).[47,48]

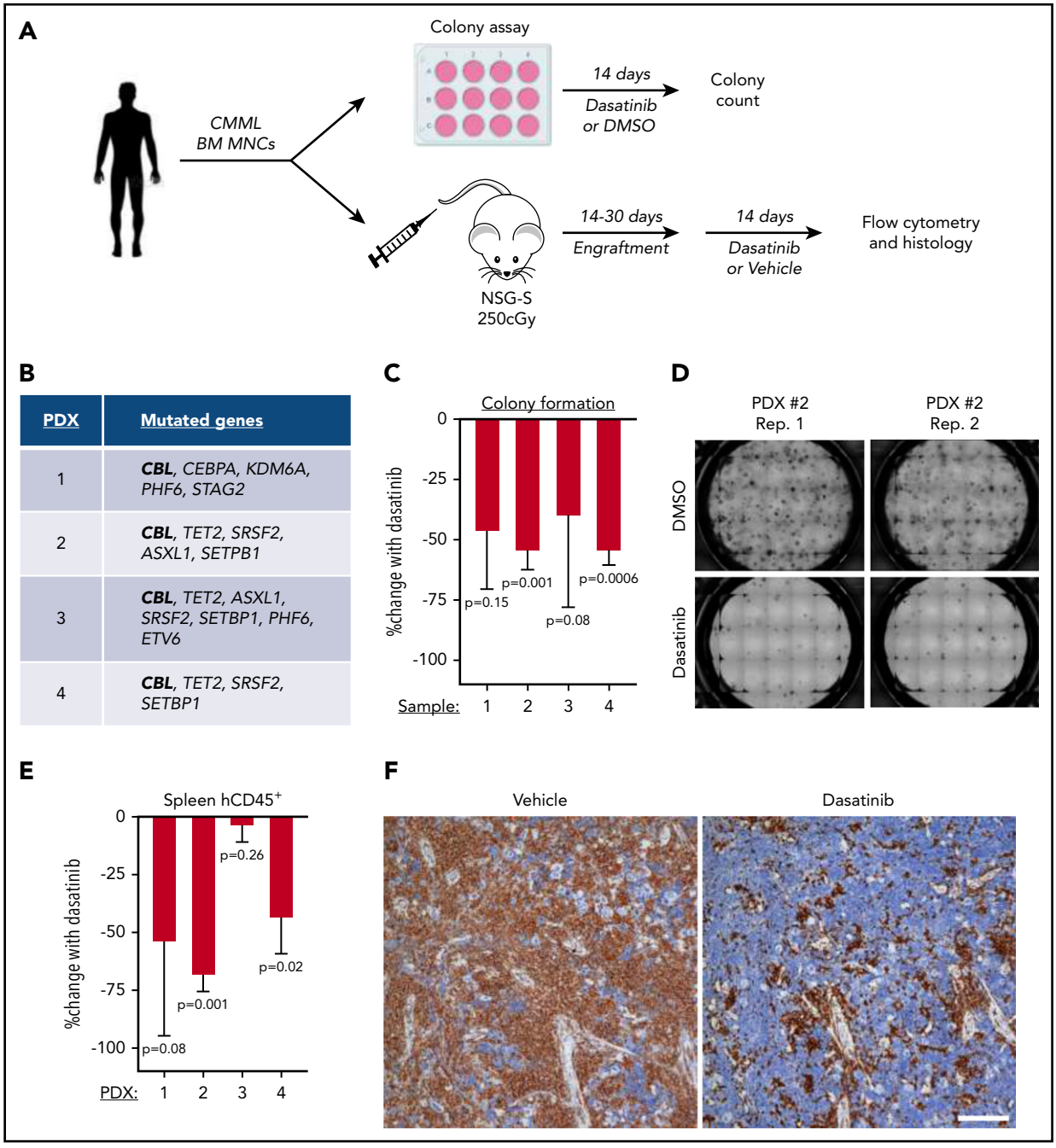

Figure 5. Dasatinib inhibits proliferation of *CBL*-mutated CMML patient samples in vitro and in vivo. (A) Schematic of the experimental workflow of CMML xenotransplantation model system. (B) Genes mutated in 4 CMML patient samples used for in vitro and in vivo experiments. (C) Percentage change in colony formation with 250 nM dasatinib compared with DMSO after 2 weeks of treatment (mean and SD of 3-4 replicate wells are depicted). (D) Representative images of colony formation by CMML patient sample 2 after 2 weeks in the presence of DMSO or 250 nM dasatinib. (E) Percentage change in human CD45$^+$ cells in the spleens of NSG-S mice engrafted with CMML patient samples and treated with vehicle or 50 mg/kg dasatinib via oral gavage over 2 weeks (mean and SD of 3-5 mice per group are depicted). (F) Anti-hCD45 immunohistochemistry in spleen tissue sections from mice engrafted with CMML patient sample 2 and treated with vehicle or dasatinib for 10 days. Anti-human CD45 stain; scale bar, 70 μM; original magnification ×100. *P* values were determined by 2-tailed Student *t* test comparing the mean for vehicle treatment to each dasatinib-treated well or mouse. BM MNC, bone marrow mononuclear cell.

The SRC-family kinase inhibitor dasatinib effectively reduced proliferation and phosphosignaling in our *CBL*-mutant cell lines, consistent with previous observations.[25,29,38,42] Interestingly, dasatinib treatment failed to reduce myeloproliferation in Cbl C379A-mutant mice,[49] an observation that might be explained by increased disease aggressiveness in mice on a mixed 129Sv/J × C57Bl/6 genetic background.[50,51] Here, we provide the first evidence that dasatinib inhibits the proliferation of a subset of patient-derived CMML samples in vitro and in vivo. Of the 8 CMML samples we tested in patient-derived xenograft (PDX) models (4 with *CBL* mutations and 4 without *CBL* mutations), dasatinib treatment reduced splenic and/or bone marrow disease burden in mice engrafted with 4 of 8 samples, including 2 *CBL* mutant and 2 *CBL* WT samples.

Mice were only treated with dasatinib once daily for 10 days prior to analysis, so it is possible that increasing the treatment period and frequency as well as the dose of dasatinib may lead to improved responses.

The effects of *CBL*-mutant expression were significantly reduced but not abolished in *Lyn*-knockout cells, indicating the presence of additional protein-protein interactions and signaling pathways involved in the gain of function conferred by *CBL* mutations; this result also highlights the likelihood that effective treatment will require combination therapy targeting multiple pathways.[24,49,52] Molecular characterization of LYN-independent signaling pathways in our model systems will reveal additional therapeutic strategies for patients with *CBL*-mutated myeloid disease.

Somatic mutations in *CBL* are typically detected in subclones that arise during disease progression.[53] *CBL* mutations can also function as disease-initiating mutations, which is evinced by the development of juvenile myelomonocytic leukemia in patients with germline *CBL* mutations[12-15]; a subset of healthy individuals with clonal hematopoiesis harbors *CBL* mutations, further suggesting that these mutations have the capacity to initiate myeloid disease.[54-56] We observed that dasatinib inhibited the proliferation of human CMML samples with either subclonal or clonal *CBL* mutations. This may indicate that *CBL*-mutant cells contribute disproportionately to colony formation in vitro or to leukemia expansion in NSG-S mice, which ultimately selects for a dasatinib-sensitive cell population. Alternatively, dasatinib may have broadly inhibitory effects on human CMML independent of the presence of *CBL* mutations. Indeed, dasatinib effectively reduced the clonogenicity and in vivo expansion of a subset of CMML samples without *CBL* mutations; these results could indicate alternative mechanisms of LYN hyperactivation or additional therapeutic targets inhibited by dasatinib in CMML.

A small clinical trial of dasatinib in 18 patients with MDS, acute myeloid leukemia, or CMML showed limited efficacy, although only 3 CMML patients were included.[57] Thus, the potential clinical benefit of dasatinib in CMML patients remains to be tested rigorously. Although the findings presented here suggest that dasatinib could be effective in CMML with gain-of-function *CBL* mutations, our results raise the possibility that a subset of CMML patients without *CBL* mutations would also respond to dasatinib. Identification of the CMML cases most sensitive to dasatinib will be further informed by characterization of the CBL-LYN-PI3K/AKT–signaling axis in patient-derived CMML samples and efficacy studies in an expanded cohort of CMML PDX models with and without *CBL* mutations.

Acknowledgments

The authors thank members of the Ebert laboratory for helpful discussions. The authors thank Traci Kruer from the Padron laboratory for providing mutational profiles for CMML samples.

This work was supported by: National Institutes of Health (NIH) National Heart, Lung, and Blood Institute grant T32HL066987 and the American Society of Hematology–Amos Medical Faculty Development Program Award (R.B.); NIH National Institute of General Medical Sciences grant T32GM007753 and NIH National Cancer Institute grant F30CA236112 (S.H.J.K.); NIH National Cancer Institute grants U24CA210986 and U01CA214125 and NIH National Institute of Diabetes and Digestive and Kidney Diseases grant U24DK112340 (S.A.C.); NIH National Cancer Institute grant R37CA234021 (E.P.); and NIH National Heart, Lung, and Blood Institute grant R01HL082945, NIH National Cancer Institute grants P01CA066996 and P50CA206963, the Howard Hughes Medical Institute, the Edward P. Evans Foundation, the Leukemia & Lymphoma Society, and the Janna Brown Charitable Trust (B.L.E.).

Authorship

Contribution: R.B. and B.L.E. conceived the study; R.B., S.H.J.K., N.D.U., A.V., M.S., E.P., and B.L.E. designed the experiments; R.B., S.H.J.K., N.D.U., A.V., L.S., T.S., C.H., M.M., V.K., A.B., C.S., and M.S. performed the experiments and/or analyzed the data; N.D.U., M.S., S.A.C., E.P., and B.L.E. supervised the work; R.B., S.H.J.K., and B.L.E. drafted the manuscript; N.D.U., S.A.C., and E.P. edited and provided feedback on the manuscript; and all authors reviewed the final version of the manuscript.

Conflict-of-interest disclosure: B.L.E. has received research funding from Celgene and Deerfield and serves on the scientific advisory boards for Skyhawk Therapeutics and Exo Therapeutics. The remaining authors declare no competing financial interests.

ORCID profiles: R.B., 0000-0001-8496-287X; S.H.J.K., 0000-0001-6482-383X; C.H., 0000-0002-6668-2222; M.S., 0000-0002-6456-8768; B.L.E., 0000-0003-0197-5451.

Correspondence: Benjamin L. Ebert, Dana-Farber Cancer Institute, Department of Medical Oncology, 450 Brookline Ave, Dana 1610A, Boston, MA 02115; e-mail: benjamin_ebert@dfci.harvard.edu.

Footnotes

Submitted 30 April 2020; accepted 14 December 2020; prepublished online on *Blood* First Edition 7 January 2021. DOI 10.1182/blood.2020006528.

*R.B. and S.H.J.K. contributed equally to this work.

For original data, please contact Benjamin L. Ebert (benjamin_ebert@dfci.harvard.edu).

The online version of this article contains a data supplement.

The publication costs of this article were defrayed in part by page charge payment. Therefore, and solely to indicate this fact, this article is hereby marked "advertisement" in accordance with 18 USC section 1734.

REFERENCES

1. Taylor J, Xiao W, Abdel-Wahab O. Diagnosis and classification of hematologic malignancies on the basis of genetics. *Blood*. 2017; 130(4):410-423.
2. Sargin B, Choudhary C, Crosetto N, et al. Flt3-dependent transformation by inactivating c-Cbl mutations in AML. *Blood*. 2007;110(3): 1004-1012.
3. Grand FH, Hidalgo-Curtis CE, Ernst T, et al. Frequent CBL mutations associated with 11q acquired uniparental disomy in myeloproliferative neoplasms. *Blood*. 2009;113(24): 6182-6192.
4. Caligiuri MA, Briesewitz R, Yu J, et al. Novel c-CBL and CBL-b ubiquitin ligase mutations in human acute myeloid leukemia. *Blood*. 2007; 110(3):1022-1024.
5. Dunbar AJ, Gondek LP, O'Keefe CL, et al. 250K single nucleotide polymorphism array karyotyping identifies acquired uniparental disomy and homozygous mutations, including novel missense substitutions of c-Cbl, in myeloid malignancies. *Cancer Res*. 2008;68(24):10349-10357.
6. Sanada M, Suzuki T, Shih LY, et al. Gain-of-function of mutated C-CBL tumour suppressor in myeloid neoplasms. *Nature*. 2009; 460(7257):904-908.

7. Papaemmanuil E, Gerstung M, Malcovati L, et al; Chronic Myeloid Disorders Working Group of the International Cancer Genome Consortium. Clinical and biological implications of driver mutations in myelodysplastic syndromes. *Blood*. 2013;122(22):3616-3627.

8. Haferlach T, Nagata Y, Grossmann V, et al. Landscape of genetic lesions in 944 patients with myelodysplastic syndromes. *Leukemia*. 2014;28(2):241-247.

9. Papaemmanuil E, Gerstung M, Bullinger L, et al. Genomic classification and prognosis in acute myeloid leukemia. *N Engl J Med*. 2016;374(23):2209-2221.

10. Meggendorfer M, Roller A, Haferlach T, et al. SRSF2 mutations in 275 cases with chronic myelomonocytic leukemia (CMML). *Blood*. 2012;120(15):3080-3088.

11. Kohlmann A, Grossmann V, Klein HU, et al. Next-generation sequencing technology reveals a characteristic pattern of molecular mutations in 72.8% of chronic myelomonocytic leukemia by detecting frequent alterations in TET2, CBL, RAS, and RUNX1. *J Clin Oncol*. 2010;28(24):3858-3865.

12. Loh ML, Sakai DS, Flotho C, et al. Mutations in CBL occur frequently in juvenile myelomonocytic leukemia. *Blood*. 2009;114(9):1859-1863.

13. Stieglitz E, Taylor-Weiner AN, Chang TY, et al. The genomic landscape of juvenile myelomonocytic leukemia. *Nat Genet*. 2015;47(11):1326-1333.

14. Murakami N, Okuno Y, Yoshida K, et al. Integrated molecular profiling of juvenile myelomonocytic leukemia. *Blood*. 2018;131(14):1576-1586.

15. Niemeyer CM, Kang MW, Shin DH, et al. Germline CBL mutations cause developmental abnormalities and predispose to juvenile myelomonocytic leukemia. *Nat Genet*. 2010;42(9):794-800.

16. Padron E, Garcia-Manero G, Patnaik MM, et al. An international data set for CMML validates prognostic scoring systems and demonstrates a need for novel prognostication strategies. *Blood Cancer J*. 2015;5(7):e333.

17. Yoshizato T, Nannya Y, Atsuta Y, et al. Genetic abnormalities in myelodysplasia and secondary acute myeloid leukemia: impact on outcome of stem cell transplantation. *Blood*. 2017;129(17):2347-2358.

18. Duchmann M, Yalniz FF, Sanna A, et al. Prognostic role of gene mutations in chronic myelomonocytic leukemia patients treated with hypomethylating agents. *EBioMedicine*. 2018;31:174-181.

19. Thien CBF, Langdon WY. Cbl: many adaptations to regulate protein tyrosine kinases. *Nat Rev Mol Cell Biol*. 2001;2(4):294-307.

20. Abbas S, Rotmans G, Löwenberg B, Valk PJM. Exon 8 splice site mutations in the gene encoding the E3-ligase CBL are associated with core binding factor acute myeloid leukemias. *Haematologica*. 2008;93(10):1595-1597.

21. Makishima H, Cazzolli H, Szpurka H, et al. Mutations of e3 ubiquitin ligase cbl family members constitute a novel common pathogenic lesion in myeloid malignancies. *J Clin Oncol*. 2009;27(36):6109-6116.

22. Rathinam C, Thien CBF, Langdon WY, Gu H, Flavell RA. The E3 ubiquitin ligase c-Cbl restricts development and functions of hematopoietic stem cells. *Genes Dev*. 2008;22(8):992-997.

23. Rathinam C, Thien CBF, Flavell RA, Langdon WY. Myeloid leukemia development in c-Cbl RING finger mutant mice is dependent on FLT3 signaling. *Cancer Cell*. 2010;18(4):341-352.

24. Nakata Y, Ueda T, Nagamachi A, et al. Acquired expression of Cbl Q367P in mice induces dysplastic myelopoiesis mimicking chronic myelomonocytic leukemia. *Blood*. 2017;129(15):2148-2160.

25. Makishima H, Sugimoto Y, Szpurka H, et al. CBL mutation-related patterns of phosphorylation and sensitivity to tyrosine kinase inhibitors. *Leukemia*. 2012;26(7):1547-1554.

26. Tezuka T, Umemori H, Fusaki N, et al. Physical and functional association of the cbl proto-oncogen product with an src-family protein tyrosine kinase, p53/56lyn, in the B cell antigen receptor-mediated signaling. *J Exp Med*. 1996;183(2):675-680.

27. Dombrosky-Ferlan PM, Corey SJ. Yeast two-hybrid in vivo association of the Src kinase Lyn with the proto-oncogene product Cbl but not with the p85 subunit of PI 3-kinase. *Oncogene*. 1997;14(17):2019-2024.

28. Grishin A, Sinha S, Roginskaya V, et al. Involvement of Shc and Cbl-PI 3-kinase in Lyn-dependent proliferative signaling pathways for G-CSF. *Oncogene*. 2000;19(1):97-105.

29. Bunda S, Qin K, Kommaraju K, Heir P, Ohh M. Juvenile myelomonocytic leukaemia-associated mutation in Cbl promotes resistance to apoptosis via the Lyn-PI3K/AKT pathway. *Oncogene*. 2015;34(6):789-797.

30. Kluk MJ, Lindsley RC, Aster JC, et al. Validation and implementation of a custom next-generation sequencing clinical assay for hematologic malignancies. *J Mol Diagn*. 2016;18(4):507-515.

31. Kahn JD, Miller PG, Silver AJ, et al. PPM1D-truncating mutations confer resistance to chemotherapy and sensitivity to PPM1D inhibition in hematopoietic cells. *Blood*. 2018;132(11):1095-1105.

32. Yoshimi A, Balasis ME, Vedder A, et al. Robust patient-derived xenografts of MDS/MPN overlap syndromes capture the unique characteristics of CMML and JMML [published correction appears in *Blood*. 2017;130(13):1602]. *Blood*. 2017;130(4):397-407.

33. Xu Y, Harder KW, Huntington ND, Hibbs ML, Tarlinton DM. Lyn tyrosine kinase: accentuating the positive and the negative. *Immunity*. 2005;22(1):9-18.

34. Hunter S, Burton EA, Wu SC, Anderson SM. Fyn associates with Cbl and phosphorylates tyrosine 731 in Cbl, a binding site for phosphatidylinositol 3-kinase. *J Biol Chem*. 1999;274(4):2097-2106.

35. Ueno H, Sasaki K, Honda H, et al. c-Cbl is tyrosine-phosphorylated by interleukin-4 and enhances mitogenic and survival signals of interleukin-4 receptor by linking with the phosphatidylinositol 3′-kinase pathway. *Blood*. 1998;91(1):46-53.

36. Bantscheff M, Eberhard D, Abraham Y, et al. Quantitative chemical proteomics reveals mechanisms of action of clinical ABL kinase inhibitors. *Nat Biotechnol*. 2007;25(9):1035-1044.

37. Nadeau SA, An W, Mohapatra BC, et al. Structural determinants of the gain-of-function phenotype of human leukemia-associated mutant CBL oncogene. *J Biol Chem*. 2017;292(9):3666-3682.

38. Bunda S, Kang MW, Sybingco SS, et al. Inhibition of SRC corrects GM-CSF hypersensitivity that underlies juvenile myelomonocytic leukemia. *Cancer Res*. 2013;73(8):2540-2550.

39. Bandi SR, Brandts C, Rensinghoff M, et al; Study Alliance Leukemias. E3 ligase-defective Cbl mutants lead to a generalized mastocytosis and myeloproliferative disease. *Blood*. 2009;114(19):4197-4208.

40. Reindl C, Quentmeier H, Petropoulos K, et al. CBL exon 8/9 mutants activate the FLT3 pathway and cluster in core binding factor/11q deletion acute myeloid leukemia/myelodysplastic syndrome subtypes. *Clin Cancer Res*. 2009;15(7):2238-2247.

41. Fernandes MS, Reddy MM, Croteau NJ, et al. Novel oncogenic mutations of CBL in human acute myeloid leukemia that activate growth and survival pathways depend on increased metabolism. *J Biol Chem*. 2010;285(42):32596-32605.

42. Javadi M, Richmond TD, Huang K, Barber DL. CBL linker region and RING finger mutations lead to enhanced granulocyte-macrophage colony-stimulating factor (GM-CSF) signaling via elevated levels of JAK2 and LYN. *J Biol Chem*. 2013;288(27):19459-19470.

43. Lv K, Jiang J, Donaghy R, et al. CBL family E3 ubiquitin ligases control JAK2 ubiquitination and stability in hematopoietic stem cells and myeloid malignancies. *Genes Dev*. 2017;31(10):1007-1023.

44. Naramura M, Nandwani N, Gu H, Band V, Band H. Rapidly fatal myeloproliferative disorders in mice with deletion of Casitas B-cell lymphoma (Cbl) and Cbl-b in hematopoietic stem cells. *Proc Natl Acad Sci USA*. 2010;107(37):16274-16279.

45. An W, Nadeau SA, Mohapatra BC, et al. Loss of Cbl and Cbl-b ubiquitin ligases abrogates hematopoietic stem cell quiescence and sensitizes leukemic disease to chemotherapy. *Oncotarget*. 2015;6(12):10498-10509.

46. Mohapatra B, Zutshi N, An W, et al. An essential role of CBL and CBL-B ubiquitin ligases in mammary stem cell maintenance. *Development*. 2017;144(6):1072-1086.

47. Robb L. Cytokine receptors and hematopoietic differentiation. *Oncogene*. 2007;26(47):6715-6723.

48. Baker SJ, Rane SG, Reddy EP. Hematopoietic cytokine receptor signaling. *Oncogene*. 2007;26(47):6724-6737.

49. Duyvestyn JM, Taylor SJ, Dagger SA, et al. Dasatinib targets B-lineage cells but does not provide an effective therapy for myeloproliferative disease in c-Cbl RING finger mutant mice. *PLoS One*. 2014;9(4):e94717.

50. Thien CBF, Blystad FD, Zhan Y, et al. Loss of c-Cbl RING finger function results in high-intensity TCR signaling and thymic deletion. *EMBO J*. 2005;24(21):3807-3819.

51. Li Q, Haigis KM, McDaniel A, et al. Hematopoiesis and leukemogenesis in mice expressing oncogenic NrasG12D from the endogenous locus. *Blood*. 2011;117(6):2022-2032.

52. Taylor SJ, Dagger SA, Thien CBF, Wikstrom ME, Langdon WY. Flt3 inhibitor AC220 is a potent therapy in a mouse model of myeloproliferative disease driven by enhanced wild-type Flt3 signaling. *Blood*. 2012;120(19):4049-4057.

53. Patel BJ, Przychodzen B, Thota S, et al. Genomic determinants of chronic myelomonocytic leukemia. *Leukemia*. 2017;31(12):2815-2823.

54. Jaiswal S, Fontanillas P, Flannick J, et al. Age-related clonal hematopoiesis associated with adverse outcomes. *N Engl J Med*. 2014;371(26):2488-2498.

55. Genovese G, Kähler AK, Handsaker RE, et al. Clonal hematopoiesis and blood-cancer risk inferred from blood DNA sequence. *N Engl J Med*. 2014;371(26):2477-2487.

56. Xie M, Lu C, Wang J, et al. Age-related mutations associated with clonal hematopoietic expansion and malignancies. *Nat Med*. 2014;20(12):1472-1478.

57. Duong VH, Jaglal MV, Zhang L, et al. Phase II pilot study of oral dasatinib in patients with higher-risk myelodysplastic syndrome (MDS) who failed conventional therapy. *Leuk Res*. 2013;37(3):300-304.